

Total inclusive hadron productions

25.1 Heavy quarkonia OZI-violating decays

In the previous chapter, we have studied the QCD jets from the OZI-violating decays of quarkonia, which occurs through the diagrams in Fig. 25.1.

OZI or Zweig rule [9,254] states that the decays of an heavy resonance involving disconnected diagrams such as in the previous figure are suppressed. In QCD, the rate behaves as α_s^3 for a spin one and to order α_s^2 for a spin zero resonance. In the case of the $\bar{b}b$ states:

$$\begin{aligned} \Upsilon &\rightarrow \text{hadrons} \sim M_\Upsilon \alpha_s^3(M_\Upsilon) \\ \eta_b &\rightarrow \text{hadrons} \sim M_{\eta_b} \alpha_s^2(M_{\eta_b}). \end{aligned} \quad (25.1)$$

The rule works better for heavier and heavier resonances, which can be understood from a $1/N_c$ argument [304]. Phenomenologically, a decay of a $\bar{Q}Q$ resonance into a $\bar{Q}Q$ pair should involve a pair of open Q states $\bar{Q}q$ and $\bar{q}Q$. As the open Q states are too heavy, there is not enough phase space for the $\bar{Q}Q$ resonance to decay into them. An explanation of the smallness of this width was one of the successes of QCD [305]. In QCD, the evaluation of the width consists of replacing the sum over hadron states by the gluons. Let's consider the $1^-(^3S_1)$ quarkonia states described by the hadronic current:

$$J_V^\mu(x) = \bar{Q}\gamma^\mu Q. \quad (25.2)$$

To lowest order of QCD, one has:

$$1^- \rightarrow \text{hadrons} \simeq 1^- \rightarrow 3g. \quad (25.3)$$

In this way, the onium decay is very similar to the one of positronium up to an overall colour factor:

$$\Gamma(V \rightarrow \text{hadrons}) \simeq \frac{64(\pi^2 - 9)}{9} C_V \frac{|\Psi_1(0)|^2}{M_V^2} \alpha_s^3(M_V^2), \quad (25.4)$$

where $|\Psi_1(0)|^2$ is the square of the onium wave function at the origin, and is proportional to the matrix element:

$$\langle V | \bar{Q}\gamma^\mu Q | 0 \rangle, \quad (25.5)$$

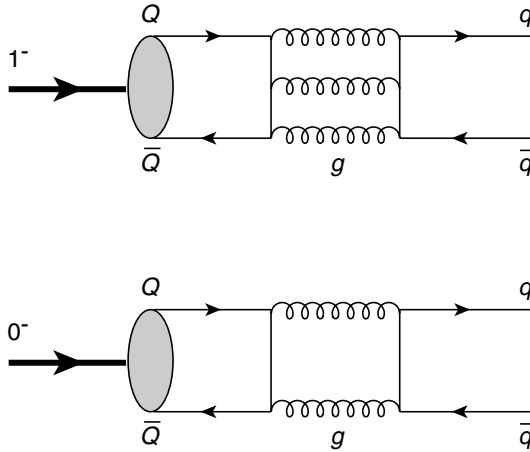


Fig. 25.1. Hadronic decays of an heavy quarkonium.

while:

$$C_V = \frac{1}{16N_c} \sum_{abc} d_{abc}^2 = 5/18 \tag{25.6}$$

is the colour factor. The wave function can be also related to the $V \rightarrow e^+e^-$ width as:

$$\Gamma(V \rightarrow e^+e^-) = \frac{16\pi Q_Q^2 \alpha^2}{M_V^2} |^3\Psi_1(0)|^2. \tag{25.7}$$

where Q_Q is the heavy quark charge in units of e . Therefore, one obtains the branching ratio:

$$R_V \equiv \frac{\Gamma(V \rightarrow \text{hadrons})}{\Gamma(V \rightarrow e^+e^-)} = \frac{10(\pi^2 - 9)}{81\pi} \frac{\alpha_s^3(M_V^2)}{Q_Q^2 \alpha^2}. \tag{25.8}$$

Including the next-to-leading order (NLO) corrections, one obtains in the \overline{MS} scheme:

$$\Gamma(V \rightarrow e^+e^-) = \Gamma(V \rightarrow e^+e^-)_{LO} \left[1 + 4C_F \left(\frac{\alpha_s}{\pi} \right) \right] \text{ in [306]}$$

$$\Gamma(V \rightarrow \text{hadrons}) = \Gamma(V \rightarrow \text{hadrons})_{LO} \left[1 - (3.8 \pm 0.5) \left(\frac{\alpha_s}{\pi} \right) \right] \text{ in [307], } \tag{25.9}$$

and therefore (for $n_f = 4$):

$$R_V = \frac{10(\pi^2 - 9)}{81\pi} \frac{\alpha_s^3(M_V^2)}{Q_Q^2 \alpha^2} \left[1 - (9.1 \pm 0.5) \left(\frac{\alpha_s}{\pi} \right) \right], \tag{25.10}$$

which is a huge coefficient correction, and requires an evaluation of the non-trivial next-to-next-leading order (NNLO) contribution. The situation is much better for the ratio [308]:

$$R_V \equiv \frac{\Gamma(V \rightarrow \gamma + \text{hadrons})}{\Gamma(V \rightarrow \text{hadrons})} = \frac{36Q_Q^2}{5} \frac{\alpha}{\alpha_s(M_V^2)} \left[1 + (2.2 \pm 0.6) \left(\frac{\alpha_s}{\pi} \right) \right], \tag{25.11}$$

where a large cancellation occurs because the leading-order amplitudes for $V \rightarrow 3g$ and $V \rightarrow gg\gamma$ are of the same nature. The decays of a pseudoscalar $0^-(^1S_0)$ state in the \overline{MS} scheme and, at the subtraction point $\nu = M_P$, are [309]:

$$\Gamma(P \rightarrow \gamma\gamma) = \frac{48\pi}{M_P^2} Q_Q^4 \alpha^2 |\Psi_0(0)|^2 \left[1 - \left(5 - \frac{\pi^2}{4} \right) C_F \left(\frac{\alpha_s}{\pi} \right) \right]$$

$$R_P \equiv \frac{\Gamma(P \rightarrow \text{hadrons})}{\Gamma(P \rightarrow \gamma\gamma)} = \frac{2}{9Q_Q^4} \frac{\alpha_s^2(M_P^2)}{\alpha^2} \left[1 + \left(\frac{\alpha_s}{\pi} \right) \left(17.13 - \frac{8}{9}n_f \right) \right] \quad (25.12)$$

and also have huge α_s corrections. In the BLM scheme [173], where the vacuum polarization corrections are absorbed into the definition of the QCD coupling (see previous chapter on the renormalizations), one can decrease the strength of the coefficient:

$$R_P^{BLM} \simeq \frac{2}{9Q_Q^4} \frac{\alpha_s^2(M^*)}{\alpha^2} \left[1 + 2.46 \left(\frac{\alpha_s}{\pi} \right) (M^*) \right], \quad (25.13)$$

but the scale at which the coupling is evaluated becomes too low $M^* \simeq 0.26M_P$. Another unclear situation is the possible effect of the analytical continuation from Euclidean (QCD result) to the time-like (the process) regions (see e.g. [310] for related discussions). These processes have been used to estimate the value of α_s from J/Ψ and Υ decays [311], after the inclusions of relativistic and finite mass corrections, and an estimate of higher-order corrections. The analysis gives:

$$\alpha_s(M_{Z^0}) = 0.113_{-0.005}^{+0.007}, \quad (25.14)$$

which is comparable with other results, although most probably, the error has been underestimated. The result needs to be confirmed by the inclusion of the NNLO terms.

25.2 Alternative extractions of α_s from heavy quarkonia

Alternative to these non-relativistic approaches, are the QCD spectral sum rule (QSSR) analysis which will be discussed in the following chapters. They have also been used to extract the QCD coupling α_s from the leptonic widths [312,155] after the resummation of Coulombic corrections. However, the result should be affected by the value of the quark mass and of the non-perturbative terms which are strongly correlated in the sum rule analysis [3,148,149,313]. The result quoted in [139] is:

$$\alpha_s(M_{Z^0}) = 0.118 \pm 0.006. \quad (25.15)$$

Using also QSSR, α_s has been extracted from the meson mass-splitting to order α_s [313], with the NLO result:

$$\frac{M_{1P_1}^2}{M_{3P_1}^2} \simeq 1 + \alpha_s(\sigma) \left[\Delta_\alpha^{13}(\text{exact}) = 0.014_{-0.004}^{+0.008} \right] + \mathcal{O}(\alpha_s^2), \quad (25.16)$$

where $\sigma^{-1} \simeq 1.3 \text{ GeV}$ is the sum rule scale. Using the experimental value $M_{\tau P_1}^2 \simeq 3526.1 \text{ GeV}$, one can deduce:

$$\alpha_s(1.3 \text{ GeV}) = 0.64_{-0.18}^{+0.36} \implies \alpha_s(M_{Z^0}) = 0.127 \pm 0.009, \quad (25.17)$$

in fair agreement with the different predictions given in the next section, although not included in the ‘world summary table’ (Table VI.1). For a comparison, one can also use non-perturbative lattice calculations of the Υ mass splittings. The resulting value of $\alpha_s(M_{Z^0})$ ranges from 0.105 ± 0.004 (quenched approximation [314]) to 0.1174 ± 0.0024 [315] and 0.1118 ± 0.0017 [316] for two dynamic quarks, indicating that systematic errors are not under good control. A more conservative lattice result has been adopted to be:

$$\alpha_s(M_{Z^0}) = 0.115 \pm 0.006, \quad (25.18)$$

as quoted in the ‘world summary table’ (Table VI.1), given in Part VI [139].

25.3 $e^+e^- \rightarrow$ hadrons total cross-section

The inclusive $e^+e^- \rightarrow$ hadrons production is the simplest though fundamental deep inelastic process. The data until LEP energies are shown in Figs. 25.2 and 25.3.

In the one photon approximation (below the Z^0 mass), the hadronic production occurs through the process shown in Fig. 25.4, in which the $\bar{q}q$ pairs interact through QCD forces, and then exchange and emit gluons in different ways.

However, we do not yet have a good understanding on the way quarks and gluons hadronize. At short distance $x \sim 1/\sqrt{t}$, one can use perturbative QCD for predicting the

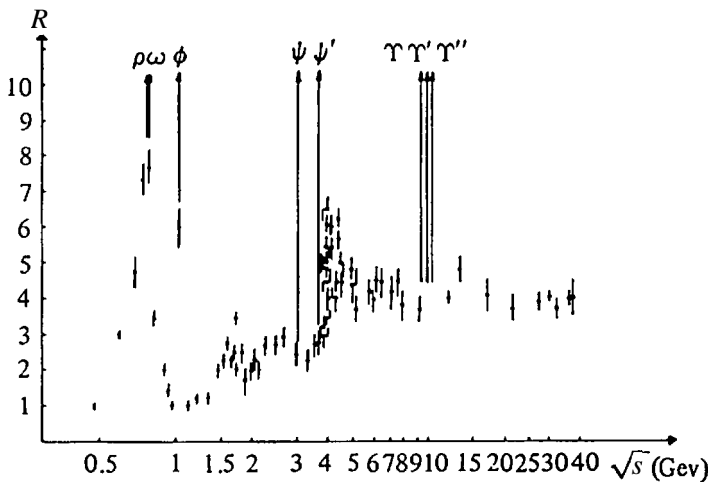


Fig. 25.2. $e^+e^- \rightarrow$ hadrons data at lower energies.

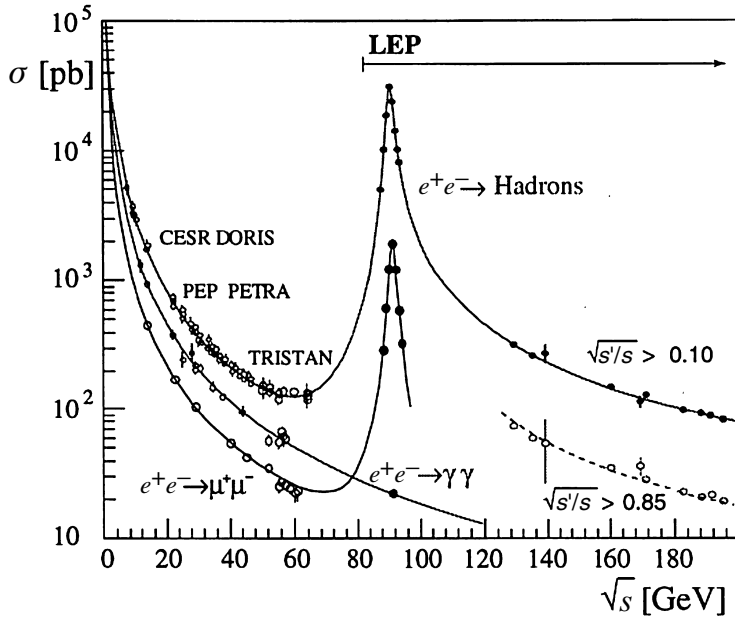


Fig. 25.3. $e^+e^- \rightarrow$ hadrons data at LEP energies.

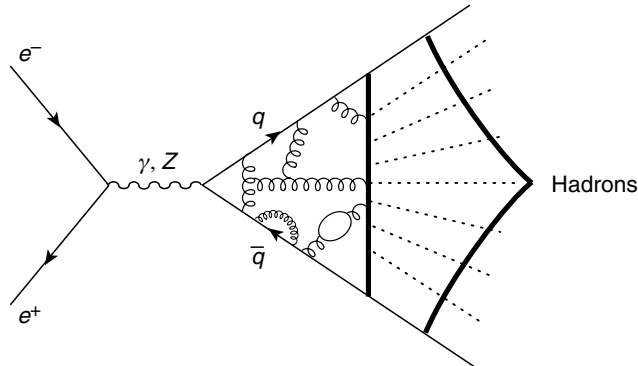


Fig. 25.4. $e^+e^- \rightarrow$ hadrons inclusive process.

total inclusive productions:

$$\sigma(e^+e^- \rightarrow \text{hadrons}) = \sigma(e^+e^- \rightarrow \bar{q}q + \bar{q}qg + \bar{q}qgg + \dots), \quad (25.19)$$

as the details of the final hadronization is irrelevant for the inclusive sum, because the probability to hadronize is one owing to the confinement assumption. Technically, one can consider the two-point function of the electromagnetic hadronic current:

$$\Pi_{\text{em}}^{\mu\nu}(q^2) = i \int d^4x e^{iqx} \langle 0 | \mathbf{T} J^\mu(x) J^{\nu\dagger}(0) | 0 \rangle = -(g^{\mu\nu} q^2 - q^\mu q^\nu) \Pi_{\text{em}}(q^2), \quad (25.20)$$

where:

$$J_\mu(x) = \frac{2}{3}\bar{u}(x)\gamma_\mu u(x) - \frac{1}{3}\bar{d}(x)\gamma_\mu d(x) - \frac{1}{3}\bar{s}(x)\gamma_\mu s(x) + \dots \tag{25.21}$$

is the electromagnetic current associated to the quarks u, d, s, \dots . Thanks to its analyticity property, $\Pi_{em}(q^2)$ obeys the well-known Källén–Lehmann dispersion relation (Hilbert representation):

$$\Pi_{em}(q^2) = \int_{t_<}^\infty \frac{dt}{t - q^2 - i\epsilon} \frac{1}{\pi} \text{Im}\Pi_{em}(t) + \dots, \tag{25.22}$$

where \dots represents subtraction terms, which are, in general, polynomial in q^2 ; $t_<$ is the hadronic threshold. Its imaginary (absorptive) part is related to the total cross-section:

$$\sigma(e^+e^- \rightarrow \text{hadrons}) = \frac{4\pi^2\alpha}{q^2} e^2 \frac{1}{\pi} \text{Im}\Pi_{em}(q^2), \tag{25.23}$$

where:

$$-3\theta(q)q^2 \frac{1}{\pi} \text{Im}\Pi_{em}(q^2) = \sum_\Gamma \langle 0 | J_{em}^\mu(0) | 0 \rangle \langle 0 | J_{\mu,em}^\dagger(0) | 0 \rangle (2\pi)^3 \delta^{(4)}(q - p_\Gamma). \tag{25.24}$$

Normalized to the $e^+e^- \rightarrow \mu^+\mu^-$ total cross-section:

$$\sigma(e^+e^- \rightarrow \mu^+\mu^-) = -\frac{4\pi^2\alpha^2}{3q^2}, \tag{25.25}$$

it reads:

$$R_{e^+e^-} \equiv \frac{\sigma(e^+e^- \rightarrow \text{hadrons})}{\sigma(e^+e^- \rightarrow \mu^+\mu^-)} = 12\pi \text{Im}\Pi_{em}(t + i\epsilon). \tag{25.26}$$

It is also convenient, in the perturbative calculation, to relate this quantity to the Adler D -function [317] defined as:

$$D(Q^2) \equiv -Q^2 \frac{d}{dQ^2} \Pi_{em}(Q^2). \tag{25.27}$$

In this way, one obtains:

$$R(t) = \frac{1}{2i\pi} \int_{-t-i\epsilon}^{t+i\epsilon} \frac{dQ^2}{Q^2} D(Q^2), \tag{25.28}$$

where it is necessary to transform the result into the physical region by taking into account the effects due to the analytic continuation of the terms of the type:

$$\ln^n(-q^2/v^2) \rightarrow (\ln(-q^2/v^2) + i\pi)^n. \tag{25.29}$$

Away from thresholds, one can neglect quark mass corrections, and obtain the perturbative series in α_s , in the \overline{MS} scheme. To order α_s^4 , one has:

$$R_{e^+e^-} = 3 \left(\sum_1^{n_f} Q_i^2 \right) [1 + F_2 a_s(t) + F_3 a_s^2(t) + F_4 a_s^3(t)] + F_4' a_s^3(t) \left(\sum_i Q_i \right)^2, \tag{25.30}$$

where:

$$\begin{aligned} F_2 &= 1 \text{ in } [318, 319] \\ F_3 &= 1.9857 - 0.1153n_f \text{ in } [317, 320] \\ F_4 &= -6.6368 - 1.2001n_f - 0.005n_f^2 \text{ in } [321] \\ F'_4 &= -1.2395 \text{ in } [321], \end{aligned} \quad (25.31)$$

where, for, for example, five flavours:

$$R_{e^+e^-} = \frac{11}{3} [1 + a_s(t) + 1.411a_s^2(t) - 12.80a_s^3(t) + \mathcal{O}(a_s^4)]. \quad (25.32)$$

The perturbative uncertainties are of the order a_s^4 and includes ambiguities related to the choice of renormalization scale and scheme, which leads to slightly different predictions for the truncated series. Because of the above functional forms of $R_{e^+e^-}$, relative errors in $R_{e^+e^-}$ lead to an absolute error in α_s of the same size:

$$\frac{\Delta R_{e^+e^-}}{R_{e^+e^-}} \sim \Delta\alpha_s, \quad (25.33)$$

such that precise measurement of $R_{e^+e^-}$ still leads to large errors in α_s . Re-analysis of PETRA and TRISTAN data in the c.m. energy range from 20 to 65 GeV, gives at NNLO [322]:

$$\alpha_s(42.4 \text{ GeV}) = 0.175 \pm 0.028 \implies \alpha_s(M_{Z_0}) = 0.126 \pm 0.022. \quad (25.34)$$

25.4 $Z \rightarrow$ hadrons

On top of the Z^0 , LEP experiments have produced a large statistical data sample that allow a precise measurement of α_s . The hadronic Z^0 width can be parametrized in a similar way:

$$R_Z \equiv \frac{\Gamma(Z^0 \rightarrow \text{hadrons})}{\Gamma(Z^0 \rightarrow e^+e^-)} = 3R_Z^{ew} \left[1 + \sum_{n \geq 1} \tilde{F}_n a_s^n(M_{Z^0}) + \mathcal{O}\left(\frac{m_f^2}{M_Z^2}\right) \right], \quad (25.35)$$

where:

$$R_Z^{ew} = \frac{\sum_i (v_i^2 + a_i^2)}{(v_e^2 + a_e^2)} (1 + \delta_{ew}) \quad (25.36)$$

contains the underlying $Z \rightarrow \sum_i \bar{q}_i q_i$ decay amplitude, v_e is the weak coupling of fermion to Z_0 ; δ_{ew} is the weak correction. The QCD correction coefficients \tilde{F}_n are slightly different from F_n due to the presence of both vector and axial-vector coupling. Combined LEP results lead to [68]:

$$R_Z = 20.768 \pm 0.024, \quad (25.37)$$

which gives:

$$\alpha_s(M_{Z^0}) = 0.124 \pm 0.004 \text{ (exp)} \pm 0.002 (M_H, M_t)^{+0.003}_{-0.001} \text{ (QCD)}, \quad (25.38)$$

where the second errors are from those from M_t and from M_H ranging from 100 to 1000 GeV. The last errors come from the scheme and scale dependences at NNLO.

25.5 Inclusive semi-hadronic τ decays

The QCD evaluation of the inclusive semi-hadronic process:

$$\tau \rightarrow \nu_\tau + \text{hadrons} \quad (25.39)$$

is diagrammatically similar to the $e^+e^- \rightarrow \text{hadrons}$ process. One puts all possible gluon and $\bar{q}q$ corrections to the QCD diagram in Fig. 25.5 and computes the sum of all partonic subprocesses. As in e^+e^- , one considers the two-point correlator:

$$\begin{aligned} \Pi_L^{\mu\nu}(q^2) &= i \int d^4x e^{iqx} \langle 0 | \mathbf{T} J_L^\mu(x) J_L^{\nu\dagger}(0) | 0 \rangle \\ &= -(g^{\mu\nu} q^2 - q^\mu q^\nu) \Pi_L^{(1)}(q^2) + q^\mu q^\nu \Pi_L^{(0)}(q^2), \end{aligned} \quad (25.40)$$

associated with the charged current:

$$J_L^\mu = \bar{u} \gamma^\mu (1 - \gamma_5) (d \cos \theta_C + s \sin \theta_C), \quad (25.41)$$

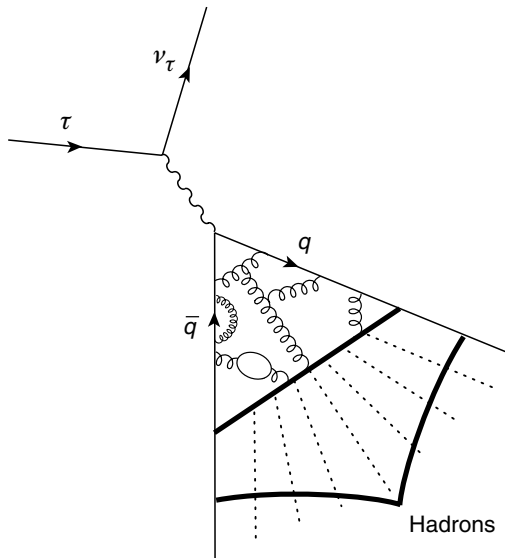


Fig. 25.5. $\tau \rightarrow \nu_\tau + \text{hadrons}$ inclusive process.

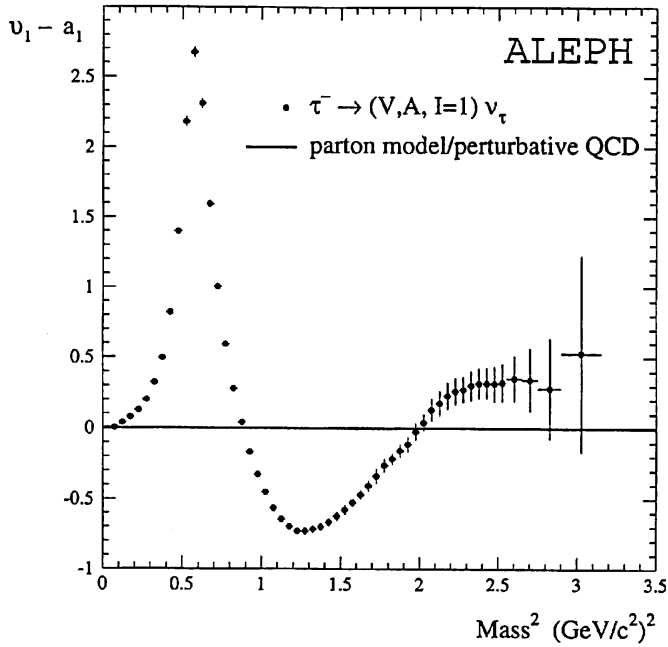


Fig. 25.6. Sum of the vector and axial-vector spectral functions from tau-decay.

where u, d and s are quark fields and θ_C is the Cabibbo angle. In terms of which, one can express the inclusive semi-hadronic branching ratio:

$$R_\tau \equiv \frac{\Gamma(\tau \rightarrow \nu_\tau + \text{hadrons})}{\Gamma(\tau \rightarrow \nu_\tau e \nu_e)} = 12\pi \int_0^{M_\tau^2} \frac{ds}{M_\tau^2} \left(1 - \frac{s}{M_\tau^2}\right)^2 \left\{ \left(1 + \frac{2s}{M_\tau^2}\right) \text{Im} \Pi_L^{(1)} + \text{Im} \Pi_L^{(0)} \right\}, \quad (25.42)$$

where [16]:

$$M_\tau = (1777.00^{+0.30}_{-0.27}) \text{ MeV}. \quad (25.43)$$

We have seen, in Part I of this book, that, in the naïve parton model, one expects:

$$R_\tau = N_c. \quad (25.44)$$

We show in Fig. 25.6 the $V + A$ spectral function measured by ALEPH.

In Fig. 14.5, we show its isovector component and a comparison with the e^+e^- data, and in Fig. 25.7, we show the difference between the vector and axial-vector spectral function.

The experimental data either from the τ -lifetime:

$$R_\tau^\Gamma \equiv \frac{\Gamma_\tau - \sum_{e,\mu} \Gamma_{\tau \rightarrow \ell}}{\Gamma_{\tau \rightarrow \ell}} \quad (25.45)$$

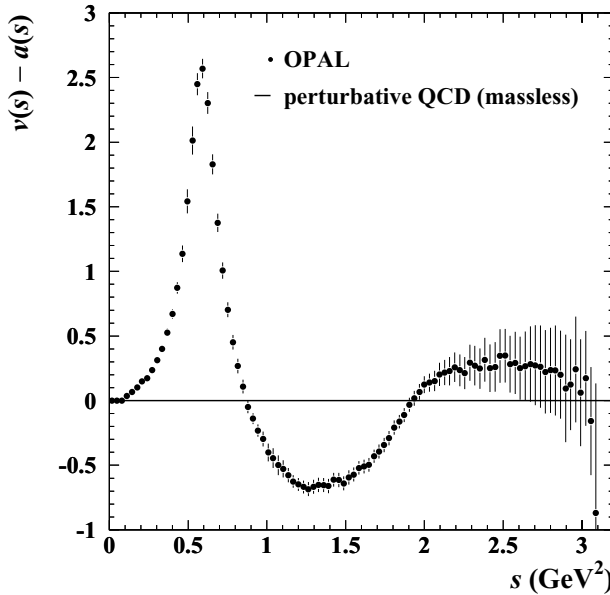


Fig. 25.7. Difference between the vector and axial-vector spectral functions from tau-decay.

or/and from the τ -leptonic branching ratios:

$$R_\tau^B \equiv \frac{1 - B_e - B_\mu}{B_e} \tag{25.46}$$

have the present average [323]:

$$R_\tau = 3.649 \pm 0.014 . \tag{25.47}$$

This experimental value is indeed a good evidence for the existence of colour but it is 20% higher than the quark-parton model estimate, such that one (a priori) can expect that QCD perturbative and/or non-perturbative corrections can resolve this discrepancy. From the expression of the width, it is clear that R_τ in Eq. (25.45) cannot be calculated directly from QCD for $s \leq \Lambda^2$. However, exploiting the analyticity of the correlators $\Pi^{(J)}$ and the Cauchy theorem, one can express R_τ as a contour integral in the complex s -plane running counter-clockwise around the circle of radius $|s| = M_\tau^2$ shown in Fig. 25.8:

$$R_\tau = 6i\pi \oint_{|s|=M_\tau^2} \frac{ds}{M_\tau^2} \left(1 - \frac{s}{M_\tau^2}\right)^2 \left\{ \left(1 + \frac{2s}{M_\tau^2}\right) \Pi_{(s)}^{(1)} + \Pi_{(s)}^{(0)} \right\} . \tag{25.48}$$

One should notice the existence of the double zero at $s = M_\tau^2$, which suppresses the uncertainties near the time-like axis. As $|s| = M_\tau^2 \gg \Lambda^2$, one can use the standard operator product expansion (OPE) à la SVZ [1] (as will be discussed in the following chapters) for the estimate of the correlators. In this way, one can express the QCD expression of the decay

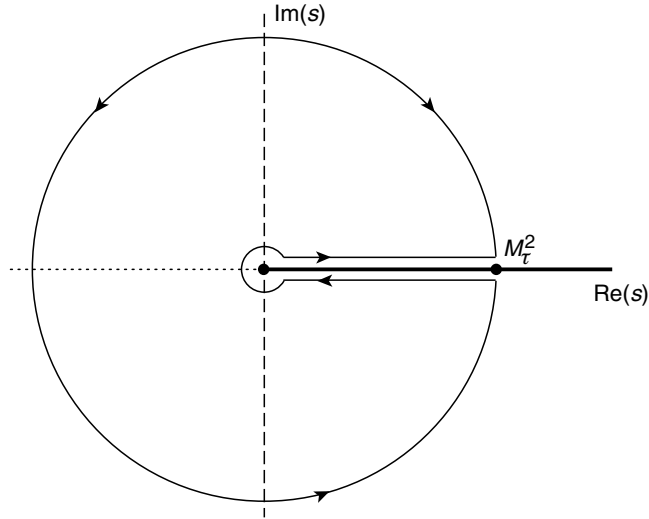


Fig. 25.8. Integration contour in the complex s -plane used to get Eq. (25.48).

width as [324] (hereafter referred to as BNP [325]):

$$R_\tau = 3(|V_{ud}|^2 + |V_{us}|^2) S_{EW} \{1 + \delta_{EW} + \delta^{(0)} + \delta_{NP}\}, \quad (25.49)$$

where:

$$|V_{ud}| \simeq 0.9753 \pm 0.0006, \quad \text{and} \quad |V_{us}| \simeq 0.221 \pm 0.003, \quad (25.50)$$

are the CKM mixing angles, while the Cabibbo angle is defined as:

$$\sin^2 \theta_C \equiv \frac{|V_{us}|^2}{|V_{ud}|^2 + |V_{us}|^2}. \quad (25.51)$$

$S_{EW} = 1.0194$ and $\delta_{EW} = 0.0010$ are LO and NLO electroweak corrections [326,327]. Based on the SVZ-Operator Product Expansion [1],¹ these non-perturbative corrections have been estimated to be small by BNP [325]:

$$\delta_{NP} \simeq -(0.7 \pm 0.4)\% \quad (25.52)$$

A direct measurement of these effects from τ decay gives [33,328]:

$$\delta_{NP} \equiv \sum_{D \geq 4} (\cos^2 \theta_c \delta_{ud}^{(D)} + \sin^2 \theta_c \delta_{us}^{(D)}) \simeq -(0.5 \pm 0.7)\%, \quad (25.53)$$

and from the most recent analysis from e^+e^- data [329] (reprinted article):²

$$\delta^{NP} \simeq -(2.8 \pm 0.6)10^{-2}, \quad (25.54)$$

¹ Here and in the rest of this section, we anticipate the discussions of the SVZ expansion and of the QCD condensates in Part VII, which the reader may consult for understanding the origin of the non-perturbative corrections.

² This result has been obtained by combining the fitted value of non-perturbative corrections in the vector channel with the theoretical estimate which relates the vector and axial-vector terms.

confirm the previous estimate of BNP. The smallness of these non-perturbative effects are related to the fact that within the SVZ expansion the numerical leading contribution behaves as $(\Lambda/M_\tau)^6$, while the radiative corrections are relatively large at the τ mass. These properties indeed show that τ decay is a good laboratory (or a *lucky process* as stated by Gabriele Veneziano) for extracting α_s . The perturbative QCD correction $\delta^{(0)}$ gives the dominant contribution, and can then be used to determine α_s at the τ -mass scale. It reads:

$$\begin{aligned} \delta_{BNP}^{(0)} &= \sum_{n=1} (K_n + g_n) a_\tau^n, \\ &= a_\tau + \left(K_2 - \frac{19}{24} \beta_1 \right) a_\tau^2 \\ &\quad + \left(K_3 - \frac{19}{12} K_2 \beta_1 - \frac{19}{24} \beta_2 + \frac{265 - 24\pi^2}{288} \beta_1^2 \right) a_\tau^3 + \mathcal{O}(a_\tau^4), \end{aligned} \quad (25.55)$$

where, here:

$$a_\tau \equiv \frac{\bar{\alpha}_s(M_\tau)}{\pi}. \quad (25.56)$$

K_n are the coefficients appearing in the D -function given in Eq. (25.31), which, for $n = 3$ flavours read:

$$K_1 \equiv F_2 = 1, \quad K_2 \equiv F_3 = 1.63982, \quad K_3 \equiv F_4 = 6.37101, \quad (25.57)$$

while g_n are induced by the contour integral and depend on $K_{m \leq n}$ and on $\beta_{m \leq n}$. For $n = 3$ flavours, one has:

$$g_2 = 3.5626, \quad g_3 = 19.9949, \quad (25.58)$$

and

$$\delta_{BNP}^{(0)} = a_\tau + 5.2023 a_\tau^2 + 26.366 a_\tau^3 + \mathcal{O}(a_\tau^4), \quad (25.59)$$

while a bold-guess of

$$K_4 \approx K_3(K_3/K_2) \approx 25, \quad (25.60)$$

confirmed by the estimate [178] ($K_4 \approx 27.5$) based on PMS [176] and ECH [177] renormalization invariant schemes, from the large β limit of QCD [330,331,154] ($K_4 \approx 24.8$) and from an experimental measurement [332] ($K_4 \approx 29 \pm 5$) gives [323]:

$$g_4 \approx 78, \quad (25.61)$$

which indicates that g_n are larger than the corresponding K_n coefficients, and implies a sizeable renormalization scale dependence [333,334]. As observed in [333], these large corrections come from the running along the circle $s = M_\tau^2 \exp(i\phi)$ ($0 \leq \phi \leq 2\pi$), which

leads to the imaginary logarithm $\log(-s/M_\tau^2) = i(\phi - \pi)$, which are large in some parts of the integration range, and leads to the *small* convergence radius $a_\tau \leq 0.11$. Using this remark, [333,335] deduce that the series is more convergent if one expands it in terms of the *contour coupling* $A^{(n)}$:

$$A^{(n)}(a_\tau) = \frac{1}{2i\pi} \oint_{|s|=M_\tau^2} \frac{ds}{s} \left(1 - 2\frac{s}{M_\tau^2} + 2\frac{s^3}{M_\tau^6} - \frac{s^4}{M_\tau^8} \right) a_\tau^n(s), \quad (25.62)$$

such that:

$$\delta^{(0)} = \sum_{n \geq 1} K_n A^{(n)}(a_\tau), \quad (25.63)$$

where the QCD series is more convergent and the renormalization scale dependence is very small [336]. The error in the truncation of the perturbative series can be estimated from the last known term of the series [337]. In this way, one can deduce the conservative estimate [323,338]:

$$\delta^{\text{trunc}} \simeq (25 \pm 50) a_\tau^4 \quad (25.64)$$

where the factor 2 has been included in the estimate of the error. In this way, the estimate of the error is about the effect of $K_3 A^{(3)}$, which appears to be conservative enough, and is, therefore, realistic. This result agrees with the one (though slightly larger) from the renormalons effect within an optimized PMS renormalization scheme, which has been estimated to be [339] (see also [340]):

$$\delta^{\text{ren}} \simeq 0.01, \quad (25.65)$$

for a typical value of $\alpha_s(M_\tau) = 0.33$. It also agrees with the fit from the e^+e^- data of the $1/M_\tau^2$ contribution [329,341]:

$$\delta^{1/M_\tau^2} \approx 0.01, \quad (25.66)$$

confirmed later on from other channels [161] (hereafter referred to as CNZ). The existence of the small $D = 2$ dimension term beyond the usual OPE expansion may be justified from the short distance linear term of the QCD potential and from monopole studies [162] as we shall see in the following chapters. The fit from e^+e^- data does not allow the existence of an eventual huge contribution from the quark constituent mass advocated sometimes in the literature, due to the small value of the contribution obtained from the fit as well as to the opposite sign compared with the expected contribution from the known coefficient of the quark mass. Indeed, the result of the fit would correspond to a tachyonic mass naturally interpreted as the one of tachyonic gluon by [161]. These results indicate that those obtained from a naïve resummation of the QCD series [331,154], [342–344] may be an overestimate of the *true* error.

Table 25.1. Values of α_s from R_τ .

Pert. Theory	ALEPH	OPAL
FOPT	0.322 ± 0.005 (exp) ± 0.019 (th)	0.324 ± 0.006 (exp) ± 0.013 (th)
CIPT	0.345 ± 0.007 (exp) ± 0.017 (th)	0.348 ± 0.010 (exp) ± 0.019 (th)
RCFT	\sim	0.306 ± 0.005 (exp) ± 0.011 (th)

Estimates of some other sources of the errors can be found in [338]. For a typical value of $R_\tau = 3.56 \pm 0.03$, these errors have been classified as follows for $\alpha_s(M_Z)$:

$$\begin{aligned}
 &0.0003 \quad \text{electroweak} \\
 &0.0010 \quad M_\tau \rightarrow M_Z \\
 &0.0005 \quad RS\text{-dependence} \\
 &0.0009 \quad \mu\text{-dependence} \\
 &0.0005 \quad \text{quark masses} \\
 &0.0009 \quad \text{SVZ condensates} \\
 &0.0014 \quad \text{truncation of the PT series at } \alpha_s^4 \\
 &\quad \text{or UV renormalon and } 1/M_\tau^2. \qquad (25.67)
 \end{aligned}$$

Adding them in quadrature, the total *theoretical* error is expected to be:

$$\Delta\alpha_s(M_Z) \simeq 0.0023, \qquad (25.68)$$

which is reflected in Table 25.1 above. The most extensive determinations of α_s from τ -decays are based on recent studies from LEP, making use of the large amount of statistical data available at LEP-1. Measurements of the vector and axial-vector differential hadronic mass distributions of τ -decays have been performed by the ALEPH and OPAL collaborations [33,328], which allow a simultaneous measurement of α_s and the non-perturbative corrections, where, as mentioned earlier, these latter are found to be small. At NNLO corrections, the resulting values of α_s from recent measurements [33] are given in Table 25.1, corresponding to the different structure of the perturbative series:

- FOPT: naïve perturbative expansion in terms of $\alpha_s(M_\tau)$ given in BNP.
- CIPT: contour-improved perturbation theory where $\delta^{(0)}$ is expressed as a contour integral in the complex- s plane.
- RCPT: renormalon chain-improved perturbation theory, where the leading terms of the β -functions are resummed by insertion of renormalon chains (gluon lines with fermion loop insertions) as will be seen in the next section.

The resulting mean value from the two experiments and from the different structure of perturbative series is:

$$\alpha_s(M_\tau) = 0.323 \pm 0.005 \text{ (exp)} \pm 0.030 \text{ (th)}, \qquad (25.69)$$

at $M_\tau = (1777.00_{-0.27}^{+0.30})$ MeV, which shows that FOPT gives the mean theoretical values. Runned to M_{Z^0} , and taking account of the different threshold effects, this value gives:

$$\alpha_s(M_{Z^0}) = 0.1181 \pm 0.0007 (\text{exp}) \pm 0.0030 (\text{th}), \quad (25.70)$$

which is in excellent agreement with the direct measurement at the Z^0 peak and with a similar error bar. This agreement of the two determinations of α_s in two extreme regime from M_τ to M_{Z^0} provides a beautiful test of the QCD prediction of the running coupling behaving as $1/\log$, which is a very significant experimental verification of asymptotic freedom.

25.5.1 Running of α_s below the τ -mass

The analysis of the running of α_s from the inclusive distribution of τ -decays [345] and from $e^+e^- \rightarrow$ hadrons data [346,329] has been extended to a lower mass below M_τ , where one does not find any deviation from the one expected from QCD. We show in Fig. 25.9 the comparison of the theoretical prediction (FOPT) and ALEPH measurements of $R_{\tau,V+A}$ for different values of the τ -mass.

In Fig. 25.10, one shows the running of $\alpha_s(s_0)$ below 3 GeV^2 using FOPT. The other structures of PT series (CIPT and RCPT) show the same behaviour [33].

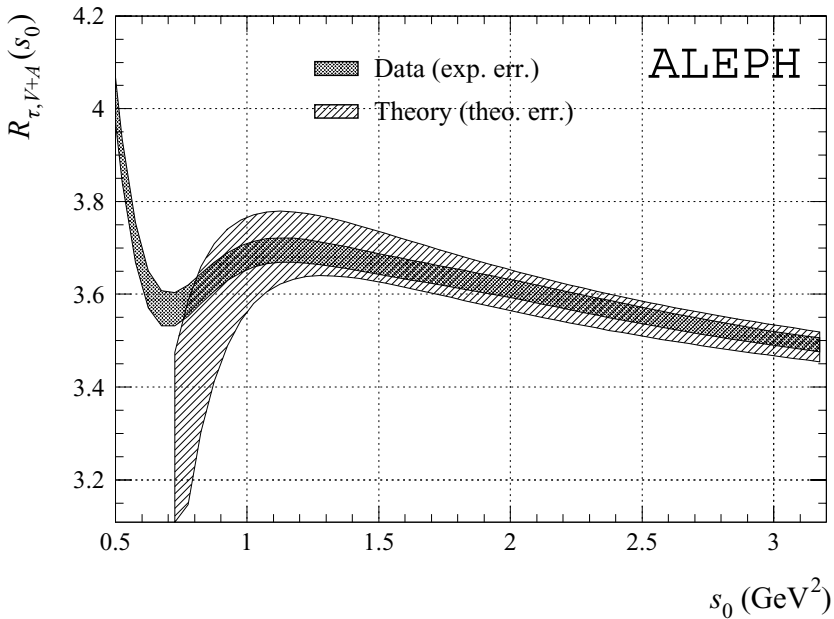


Fig. 25.9. $R_{\tau,V+A}$ as a function of the τ mass s_0 . The theoretical predictions is from FOPT.

Table 25.2. Values of α_s from different observables in τ -decays.

Observables	$\alpha_s (M_\tau^2)$
$R_{\tau,V} = 1.78 \pm 0.03$	0.35 ± 0.05
$R_{\tau,A} = 1.67 \pm 0.03$	0.34 ± 0.05
$R_{\tau,\text{excl}} = 3.58 \pm 0.05$	0.34 ± 0.04

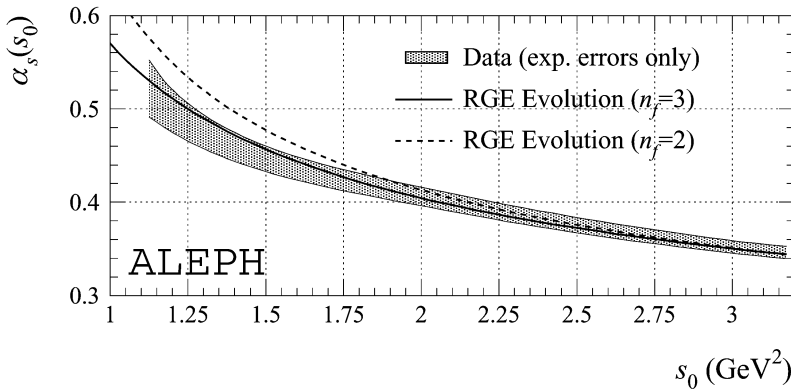


Fig. 25.10. Running of α_s from the theoretical predictions of $R_{\tau,V+A}$ from FOPT to four-loop RGE evolution for two and three flavours. The shaded band is the data.

25.6 Some other τ -like processes

25.6.1 α_s from other τ widths

One can also extend the previous analysis in order to extract the value of α_s from the vector, axial-vector and from the sum of the exclusive modes by applying a $SU(2)$ isospin rotation [347]. This analysis has been done in [338] using the compilation of data in [346]. The analysis and predictions are summarized in Table 25.2 from [338] where one should remark that the errors in each separate channel are larger than in the total inclusive mode, which comes from the fact that the non-perturbative contributions have larger errors in each separate vector and axial-vector channel than in the sum. Indeed, from [338], one can deduce the sum of the non-perturbative terms in each channel at the τ mass:

$$\delta_{NP}^V \simeq (2.4 \pm 1.3)10^{-2}, \quad \delta_{NP}^A \simeq -(4.4 \pm 2.1)10^{-2}. \quad (25.71)$$

The larger error from the exclusive modes is mainly due to the data. These different determinations are consistent with each others. In Fig. 25.11, we show the behaviour of the vector and axial-vector components of τ decays versus an hypothetical heavy lepton of mass $\sqrt{s_0}$.

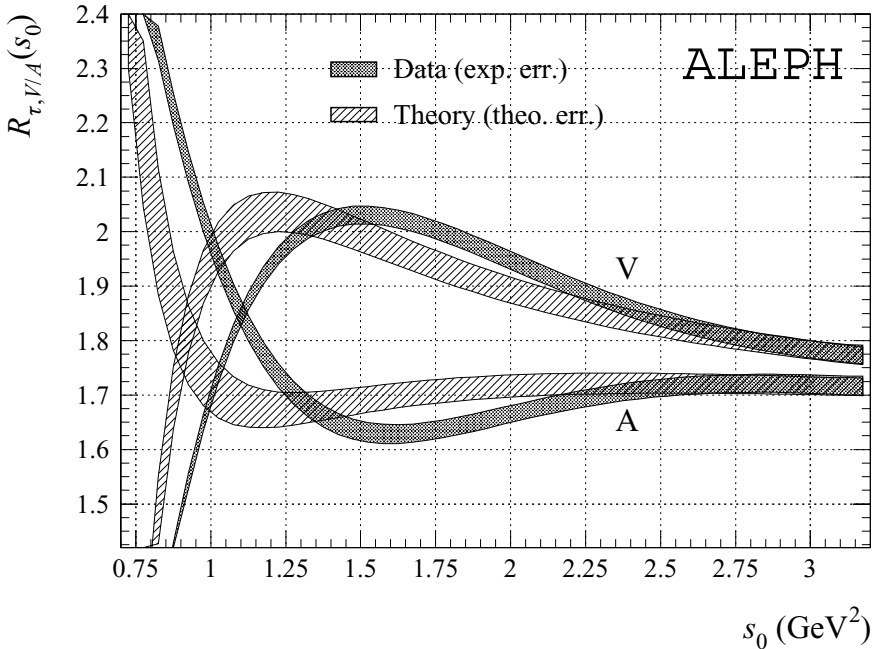


Fig. 25.11. Behaviour of $R_{\tau,V/A}$ versus the τ mass s_0 . The theoretical prediction is from FOPT.

One can again notice that the pQCD prediction is in very good agreement with the data for a value of s_0 above 1 GeV^2 , confirming that the determination of α_s from τ decays is robust.

25.6.2 α_s from $e^+e^- \rightarrow I = 1$ hadrons data

We have discussed that the vector component of the τ decay can provide an estimate of α_s although the accuracy is less than in the case of the total inclusive mode. Equivalently, one can use the e^+e^- data into the vector spectral function using an isospin rotation [347] in order to estimate α_s . In this way, the decay width reads [346]:

$$R_{\tau,V} \equiv \frac{3 \cos^2 \theta_c}{2\pi\alpha^2} S_{EW} \int_0^{M_\tau^2} ds \left(1 - \frac{s}{M_\tau^2}\right)^2 \left(1 + \frac{2s}{M_\tau^2}\right) \frac{s}{M_\tau^2} \sigma_{e^+e^- \rightarrow I=1} . \quad (25.72)$$

This quantity has been used for studying the mass dependence of the prediction on α_s . Therefore, it can provide an independent test on the reliability of the result from τ decays and a test of the isospin symmetry. The value of α_s obtained in this way [346,338,329], at the observed value of the τ mass, is given in Table 25.2. From this analysis we conclude that the e^+e^- data give a value of α_s compatible with the one from τ decay data. We show in Fig. 25.12, the behaviour of $R_{\tau,1}$ versus the value of the τ mass using FOPT.

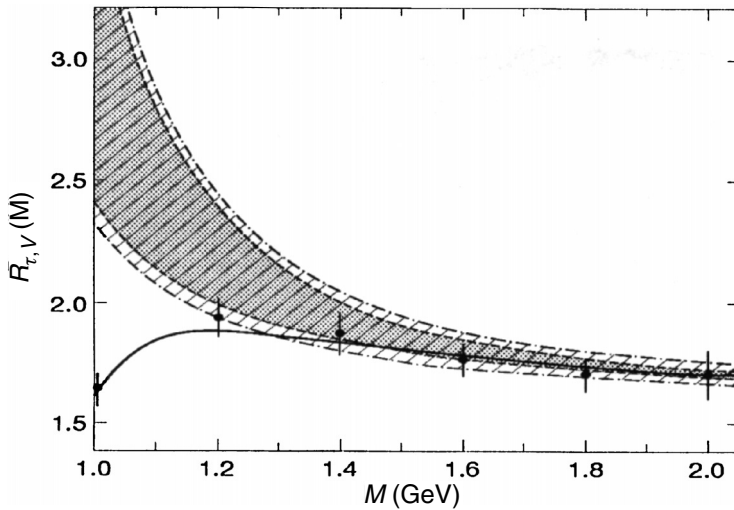


Fig. 25.12. $R_{\tau,V}$ versus the hypothetical τ mass M using e^+e^- data. The shaded region is the theoretical predictions corresponding to the choice of parameters discussed in the text.

There is a good agreement between the data and the theory above 1.2 GeV. The shaded area between the two dashed curves corresponds to the theoretical predictions for $\alpha_s(M_\tau^2) = 0.33$. The bigger allowed region at low value of M is due to the uncertainty in the leading non-perturbative contribution taken to be:

$$\delta_V^{D=6}(M) \simeq (2.4 \pm 1.3)10^{-2} \times \left(\frac{M_\tau}{M}\right)^6, \tag{25.73}$$

as given in Eq. 25.71. The departure of the theoretical prediction from the data points below 1.2 GeV signals the important role of higher dimension non-perturbative contributions which we shall discuss in the part of this book dedicated to QCD spectral sum rules. Here, a reasonable fit represented by the continuous line corresponds to the choice:

$$\alpha_s(M_\tau^2) = 0.33, \quad \delta_V^{D=6}(M_\tau^2) \simeq 2.4 \times 10^{-2}, \quad \delta_V^{D=8}(M_\tau^2) \simeq -9.5 \times 10^{-3}. \tag{25.74}$$

However, though the $D = 8$ condensate contribution is tiny at the τ mass, its effect at 1.2 GeV is 1.25 larger than the one of $D = 6$, which changes completely the shape of the QCD prediction and can raise some doubt on the validity of the OPE at this scale.

25.6.3 Strange quark mass from τ -like processes

τ -like processes have also been used for extracting the strange quark running mass defined in the previous chapter. These processes are:

- The Cabibbo suppressed transition $\Delta S = 1$ measured in [33,328] and exploited in [348]:

$$\tau \rightarrow \nu_\tau + \Delta S = 1 \text{ hadrons} \quad (25.75)$$

- The $I = 0$ $e^+e^- \rightarrow$ hadrons process:

$$e^+e^- \rightarrow I = 0 \text{ hadrons} \quad (25.76)$$

using the τ -like decay process [354] (see also [355]):

$$R_{\tau,0} \equiv \frac{3 \cos^2 \theta_c}{2\pi \alpha^2} S_{EW} \int_0^{M_\tau^2} ds \left(1 - \frac{s}{M_\tau^2}\right)^2 \left(1 + \frac{2s}{M_\tau^2}\right) \frac{s}{M_\tau^2} \sigma_{e^+e^- \rightarrow I=0} . \quad (25.77)$$

involving the $I = 0$ total cross-section or/and of its different combinations.

We shall discuss in details these processes in the chapter on quark masses.